Recent advances in spin chemistry*
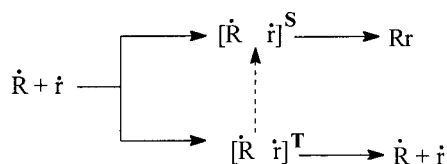
Anatoly L. Buchachenko

N. N. Semenov Institute of Chemical Physics Russian Academy of Sciences, 4 Kosygin str., 117334 Moscow, Russia

Abstract: The great success in controlling chemical reactivity by spin manipulation was achieved in the last decade, and many remarkable spin and magnetic phenomena have been discovered. Among those discoveries, the most chemically important highlights are magnetic isotope effect, spin catalysis, and single-spin tunneling spectroscopy. This paper summarizes recent advances in these new and hot areas of modern chemistry.
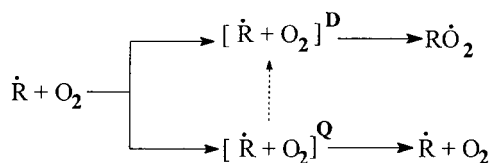
GENERAL OUTLOOK OF SPIN CHEMISTRY

Spin chemistry as a new land and hot area in modern chemistry is based on the universal and fundamental principle—all chemical reactions are spin selective. They allowed only for those spin states of products whose total electron spin is identical to that of reagents. The reactions are forbidden if they require a change of spin.

Some typical examples of spin-selective reactions are given below. The recombination of radicals into the diamagnetic molecule is allowed from singlet state of the reaction precursor, radical pair:

$$\dot{R} + \dot{r} \longrightarrow \begin{cases} [\dot{R} \quad \dot{r}]^{S} \longrightarrow Rr \\ [\dot{R} \quad \dot{r}]^{T} \longrightarrow \dot{R} + \dot{r} \end{cases}$$

Triplet state is strictly forbidden for the reaction, so that triplet pair either dissociates to free radicals, or experiences *spin conversion* (shown by dashed arrow), which transforms nonreactive triplet state into the chemically reactive singlet state.

Chemical addition of radical to triplet molecule (oxygen, for instance), as well as physical quenching of excited triplet molecule by radical, takes place only in doublet state:

$$\dot{R} + O_2 \longrightarrow \begin{cases} [\dot{R} + O_2]^{D} \longrightarrow R\dot{O}_2 \\ [\dot{R} + O_2]^{Q} \longrightarrow \dot{R} + O_2 \end{cases}$$

Quartet spin state is forbidden to react and quartet-doublet *spin conversion* is required to switch over the reaction channel. Again, spin selectivity is controlled by competition between the dissociation of the quartet pair on the starting reagents and spin transformation of the pair into the reactive doublet state.

In the reaction of two triplets (recombination of carbenes, delayed fluorescence from the fusion of two excited triplet molecules, etc.) only one of the nine spin states is open to react:

A. L. BUCHACHENKO
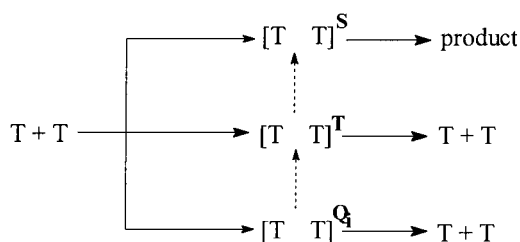
The other eight triplet and quintet spin states are forbidden for the reaction, and only *spin conversion* is able to stimulate their chemical reactivity and to switch over the reaction channel. And again, spin conversion competes with dissociation of T and Q_i pairs.

Spin chemistry is unique because it introduces in chemistry magnetic interactions. Contributing almost nothing in chemical energy, being negligibly small and traditionally ignored, magnetic interactions produce *spin conversion* and switch over the reaction from spin forbidden to spin-allowed channels (or *vice versa*). Ultimately, they implement a spin control of the reactions, they modify chemical reactivity of the reagents, and they write a new, *magnetic scenario of chemical reactions.*

All remarkable phenomena in spin chemistry, *the acts of the magnetic scenario*, may be exemplified by the radical pair which plays in spin chemistry testifying role similar to that of H_2 in quantum chemistry. Radical pair functions as an *electron* and *nuclear spin selective microreactor* in which spin conversion of nonreactive states into the chemically reactive ones is controlled by Zeeman and Fermi interactions, and microwaves (Fig. 1).

The rate of spin conversion and, therefore, the probability of the reaction (e.g., recombination) of the pair P is a function of magnetic field H, hyperfine coupling constant a, nuclear spin I and nuclear magnetic moment μ_n, nuclear spin projection m_I, resonance frequency ω and amplitude H_1 of microwaves, the energy J of exchange interradical interaction in pair. The dependence of P on these parameters generates numerous magnetic phenomena in chemistry:
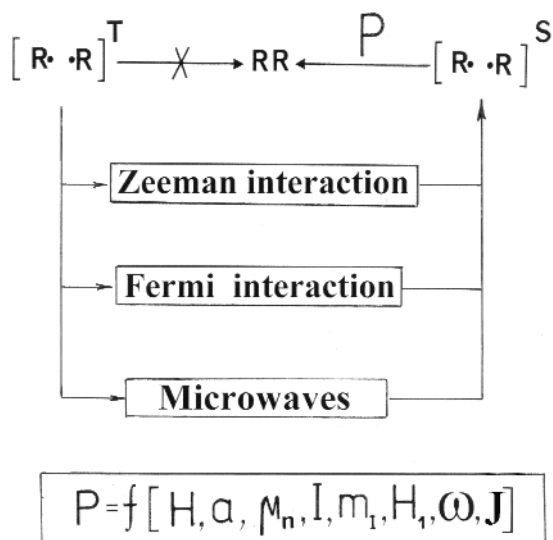
Fig. 1 General scheme of spin conversion induced by Zeeman and Fermi interactions and microwaves. Radical pair functions as a spin-selective microreactor in which the reaction probability P is a function of magnetic parameters of the radicals (a, μ_n, I_n, m_I), magnetic fields (H, H_1, ω), and exchange interaction J.

- magnetic field effect
- magnetic isotope effect
- chemically induced nuclear polarization
- chemically induced electron polarization
- radiowave emission of chemical reactions
- chemically detected magnetic resonance
- optically detected magnetic resonance
- microwave-induced magnetic isotope effect
- microwave-stimulated nuclear polarization
- spin coherency in chemical reactivity
- spin catalysis
- single-spin tunneling spectroscopy

In this paper, I will focus the reader's attention on the three of the most outstanding, significant (for chemistry), and famous phenomena—magnetic isotope effect, spin catalysis, and single-spin tunneling spectroscopy.

MAGNETIC ISOTOPE EFFECT

Discovery of magnetic isotope effect (MIE) is one of the greatest events in modern chemistry [1], comparable in importance only with that of classical, mass-dependent isotope effect (CIE). In contrast to CIE, MIE demonstrates dependence of the reaction rates on the nuclear spin, magnetic moments, and hyperfine, electron-nuclear interaction in reagents. It sorts isotope nuclei and directs them into the different reaction products according to their spin and magnetic moment. MIE results in fractionation of magnetic and nonmagnetic isotopes in chemical processes, geochemistry, and space chemistry. Now it is evident that the monitoring of contents and isotope distribution in ores, minerals, oils, coals, and space matter should take into account both mechanisms of isotope fractionation, CIE and MIE on a par, in order to accurately reconstruct genesis and pathways of chemical evolution of substances in nature. MIE may also operate in biochemical processes, so it can be considered a mechanistic tool in biochemistry. Being a phenomenon of fundamental importance, MIE offers a new tool for probing and testifying the reaction mechanisms, kinetics, and chemical physics of reactions. It can arise in spin-selective reactions of carbenes, triplet molecules, ions, and high-spin species, so that radical pair is not the only source of MIE [2].

MIE-induced isotope sorting can be illustrated by the photolysis of dibenzyl ketone, which is known to occur via fragmentation of triplet molecule and generation of triplet radical pair (Fig. 2).

Triplet–singlet conversion of magnetic pairs (with ^{13}C nuclei) is much faster than that of nonmagnetic pairs (with ^{12}C nuclei), so that magnetic pairs predominantly recombine and regenerate the
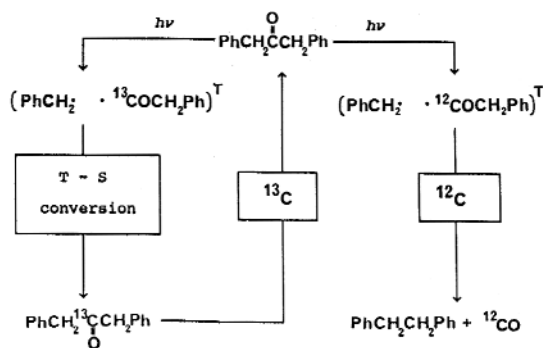

Fig. 2 Scheme of chemically induced isotope fractionation in the photolysis of dibenzylketone.

starting ketone molecules, while the delay of spin conversion of nonmagnetic pairs favors their dissociation and transformation into the reaction products. As a result, the regenerated ketone molecules accumulate ^{13}C nuclei. Thus, due to the difference in the rates of spin conversion radical pair sorts the nuclei according to their magnetic moments and dispatches magnetic and nonmagnetic nuclei into the different reaction products.

Discovery of MIE in the photolysis of dibenzyl ketone made this reaction famous and popular; physics and chemistry of MIE have been extensively studied; physical and kinetic theories of MIE have been experimentally tested by this key reaction [3].

Oxygen MIE was discovered in the reactions of chain oxidation of polymers and hydrocarbons by molecular oxygen [4]. Two reactions in the chain process are spin selective—the chain termination reaction (e.g., recombination of peroxyradicals),and chain propagation reaction (e.g., the addition of molecular oxygen to alkyl radicals). The former dominates in solid-state polymer oxidation, the latter prevails in the liquid-phase oxidation.

The scheme of isotope sorting in the termination step is shown in Fig. 3. The encounter pair of freely diffusing peroxy radicals either recombines resulting unstable tetraoxide RO_4R, which decomposes, regenerating an oxygen molecule from central oxygen atoms, or dissociates regenerating peroxy
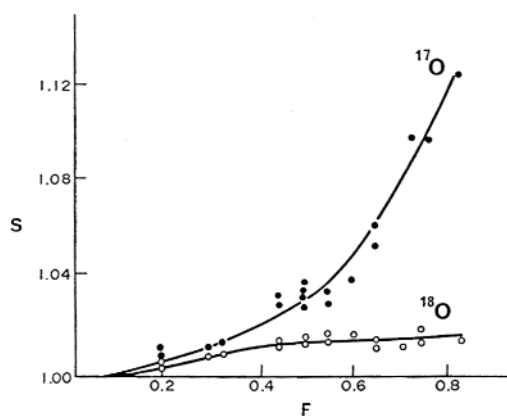
Fig. 3 Oxygen MIE and ^{17}O enrichment of molecular oxygen in the radical chain termination reaction of polymer oxidation as a function of chemical conversion of oxygen.
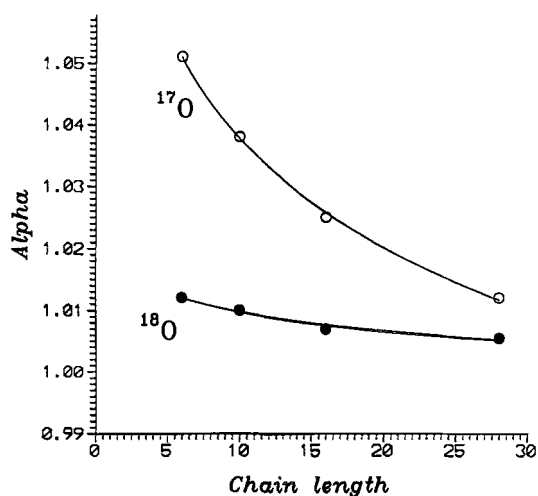

Fig. 4 ^{17}O isotope enrichment as a function of chain length in γ-initiated polyethylene oxidation.

radicals. Due to MIE, which differentiates the rates of spin conversion, the recombination probability of peroxy radicals with terminal ^{17}O atoms is higher than that of radicals with ^{16}O and ^{18}O atoms. As a result, the tetraoxide and, consequently, the recovered oxygen is enriched with ^{17}O, while the hydroperoxide molecules are enriched with ^{16}O and ^{18}O. Figure 3 demonstrates isotope enrichment of molecular oxygen as a function of oxygen conversion; the higher chemical conversion the larger number of recovered oxygen molecules and the higher isotope enrichment. It is impressive that MIE-induced ^{17}O isotope enrichment strongly exceeds ^{18}O enrichment induced by CIE.

Figure 4 shows the chain length effect on the isotope separation which evidences in favor of the mechanism of isotope selection: the shorter the chain length, the more spin-selective termination reactions and, therefore, the higher isotope sorting. Figure 5 demonstrates the impressive distinction of the temperature behavior of isotope fractionation induced by MIE and CIE.

In contrast to CIE, which exhibits only small temperature dependence (in agreement with its physical nature), MIE reveals a severe dependence; the maximum MIE reflects the most favorable conditions for isotope selection when the timescale of molecular dynamics is compatible with that of spin dynamics, providing the best nuclear spin selection in radical pair [5].

In liquid-phase oxidation, the dominating reaction responsible for oxygen isotope fractionation is the propagation reaction

$$\dot{R} + O_2 \xrightleftharpoons{k} [\dot{R}...O_2] \longrightarrow R\dot{O}_2$$
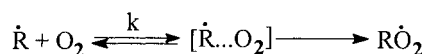
The reaction product, doublet spin state peroxy radical, originates only from the doublet pair [R˙...O2]; the quartet spin states of the pair are forbidden to react. MIE in quartet-doublet spin conversion selects magnetic ^{17}O nuclei into peroxy radicals, resulting in impoverishment of the remaining molecular oxygen with ^{17}O. In contrast, oxygen molecules with ^{18}O react slower than those with ^{16}O, resulting in CIE-induced enrichment of molecular oxygen with ^{18}O. Experiment has perfectly confirmed these predictions (Fig. 6); the ratio of the radical addition rate constants is found to be

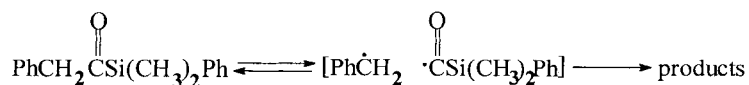$$k(^{17}O^{16}O)/k(^{16}O^{16}O) = 1.011; \quad k(^{18}O^{16}O)/k(^{16}O^{16}O) = 0.990$$

that is, $^{17}O^{16}O$ molecules react 1.1% faster than $^{16}O_2$ molecules, but $^{18}O^{16}O$ molecules react 1.0% slower than $^{16}O_2$ molecules. The former is due to MIE, the latter is induced by CIE [5].
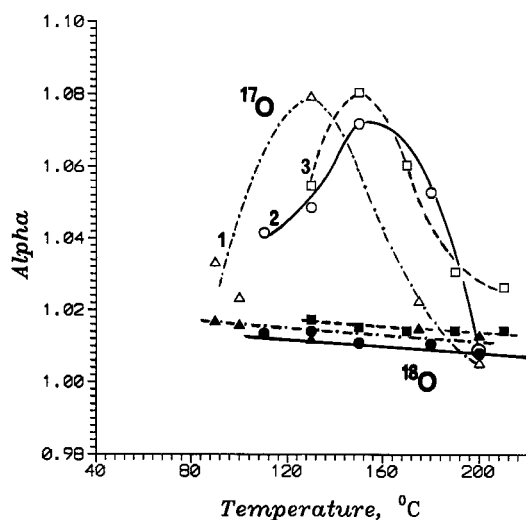
**Fig. 5** Temperature dependence of ^{17}O and ^{18}O isotope enrichment in oxidation of polyethylene (1), polypropylene (2) and polymethylpentene (3). Open circles, squares, and triangles correspond to ^{17}O; the filled ones, to ^{18}O.

^{29}Si MIE has been demonstrated in the photolysis of silylketone according to the scheme [6]:

$$\text{PhCH}_2\overset{\overset{\displaystyle O}{\|}}{\text{C}}\text{Si(CH}_3)_2\text{Ph} \xrightleftharpoons{} [\text{PhĊH}_2 \quad \cdot\overset{\overset{\displaystyle O}{\|}}{\text{C}}\text{Si(CH}_3)_2\text{Ph}] \longrightarrow \text{products}$$

which was verified by CIDNP and by inspection of the photolysis products. In triplet-sensitized photolysis, MIE in triplet radical pair selects magnetic ^{29}Si nuclei and provides an enrichment of recovered ketone with ^{29}Si isotope (Fig. 7). The other impressive result is that the inversion of the spin multiplicity of radical pair (in direct photolysis, which occurs in singlet excited state of ketone) is accompanied by inversion of the sign of MIE: ^{29}Si enrichment is replaced by small, however, reliably measured impoverishment (Fig. 7).
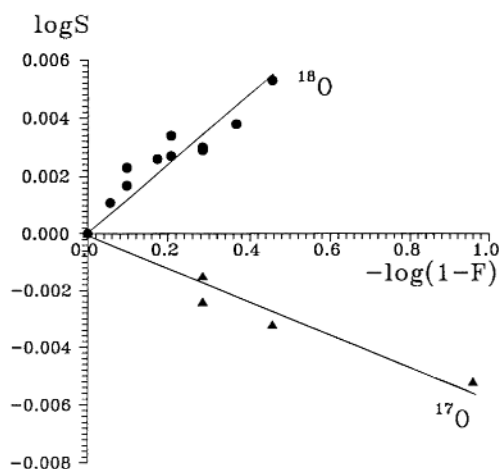

Fig. 6 Oxygen isotope fractionation in the chain propagation reaction of ethylbenzene oxidation by molecular oxygen; *S* is the isotope enrichment, *1-F* is oxygen chemical conversion.
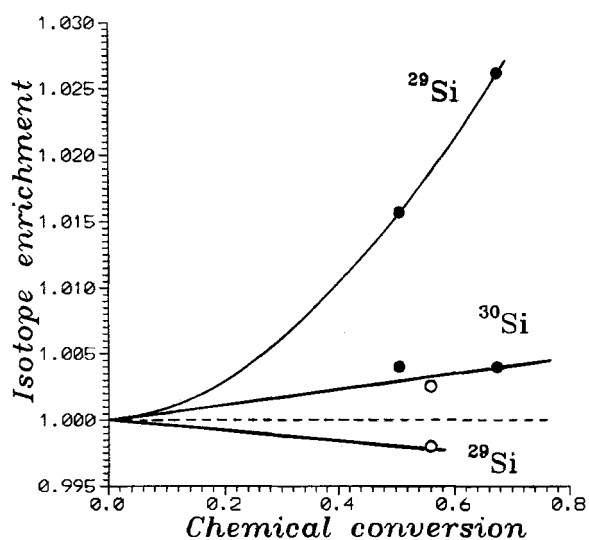
Fig. 7 Silicon isotope fractionation induced by photolysis of silyl ketone as a function of chemical conversion. CIE-induced fractionation of ^{30}Si is identical for both singlet and triplet channels of photolysis; MIE-induced ^{29}Si isotope separation is sensitive to the spin multiplicity of channels.

Now one can summarize qualitative symptoms of MIE in comparison with CIE (Table 1); they are specific and clearly contrasting for both effects.

Figure 8 illustrates the origin of [33]S MIE in direct photolysis of sulfur-containing ketone, which has been proved by CIDNP to occur via triplet radical pair according to scheme:

$$PhCCH_2SO_2Ph \underset{\longleftarrow}{\longrightarrow} [Ph\overset{O}{C}CH_2 \ \cdot SO_2Ph] \longrightarrow products$$
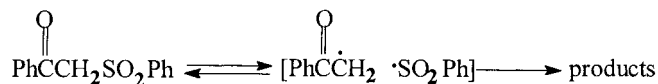
Hyperfine coupling with magnetic [33]S nuclei induces triplet–singlet conversion of the radical pair and stimulates regeneration of the starting ketone, which accumulates magnetic isotope as far as ketone itself is exhausted (Fig. 8) [8,9].

Uranium MIE has been observed in the photoreduction of uranyl salts (perchlorate, in particular) in presence of substituted phenols (Fig. 9).

The intermediate triplet radical pair, composed of uranoyl and phenoxyl radicals, regenerates the starting uranyl ion via triplet–singlet conversion if the pair contains magnetic [235]U nuclei.

The pairs with [238]U nuclei have a little chance to experience spin conversion, so they react further into the products of U^{+4} ions (unsoluble UF_4 in the presence of NH_4F, for instance) [8,9].

Table 1 MIE versus CIE: quality.

Symptoms	MIE	CIE
Selection parameters	nuclear spin and magnetic moment	nuclear mass
Fermi interaction	dependent	independent
Magnetic field	strong dependence	no dependence
Molecular dynamics	strong impact	no influence
Radical lifetime	dependent	independent
Temperature dependence	strong	very weak
Reagent spin multiplicity	strong dependence both in sign and magnitude	no influence
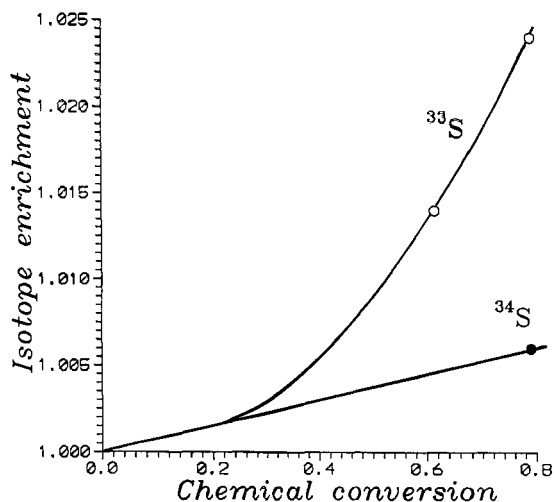
Fig. 8 Sulfur isotope fractionation induced by photolysis of sulfur-containing ketone.

The quantitative measure of MIE is a one-step enrichment coefficient α, e.g., the ratio of the reaction rates of molecules with magnetic and nonmagnetic nuclei. The kinetic scheme of partly reversible reactions (the majority of the reactions exhibiting MIE are those) can be presented by equations

$$A \underset{P}{\rightleftarrows} RP \xrightarrow{\ 1-P\ } products$$

$$A^* \underset{P^*}{\rightleftarrows} RP^* \xrightarrow{\ 1-P^*\ } products$$
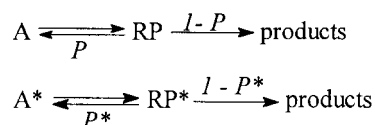
where A and A* are starting molecules, RP denotes radical pair, P and P^* are the regeneration probabilities of the starting molecules; the stars refer to the species with magnetic nuclei. Then it is very easy to derive the expression for α

$$\alpha = \frac{1-P}{1-P^*} \tag{1}$$

as well as equations which couple α with experimentally measured isotope content S and chemical conversions F and F^*:

$$S = \frac{1-F^*}{1-F} \tag{2}$$

$$\alpha = \frac{ln(1-F)}{ln(1-F^*)} \tag{3}$$

Figure 10 summarizes the α values for all magnetic isotope effects currently known. It demonstrates also that MIE is quantitatively much higher than CIE.

Now one can easily formulate a theoretical limit of nuclear spin selectivity. It follows from eq 1: an extreme α value ($\alpha = \infty$) is achieved under conditions $P = 0$ and $P^* = 1$, which implies that only magnetic radical pairs necessarily recombine and regenerate molecules, but nonmagnetic pairs are not able to regenerate starting molecules resulting in the reaction products. This limit characterizes the top nuclear spin selectivity equivalent to the chemically induced isotope purification.

Recently, two strategies have been formulated to reach this limit—cascade strategy of spin-selective reactions in confined microreactors and selective microwave pumping of magnetic or nonmagnetic radical pairs. The scheme of the cascade process shown in Fig. 11 implies multiple repetition of the cycle: excitation of molecule into the triplet state, dissociation into the triplet radical pair, triplet–singlet conversion, and regeneration of starting molecule. Each cycle of the cascade process is accompanied by nuclear, spin-selective renaissance of the molecule after its dissociation and results in accumulation of magnetic isotope in the regenerated molecules. The theory of the cascade nuclear selection has been developed, and the summary of equations derived from kinetics and statistics of the cascade process are presented in Fig. 12. They allow to find important cascade parameters n^* and n, characterizing the number of cascade cycles which magnetic and nonmagnetic molecules suffer during their survival time [10].
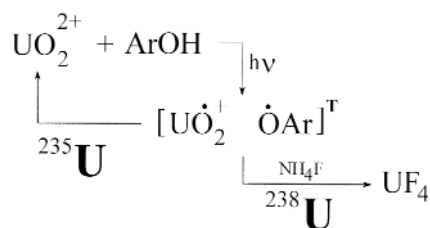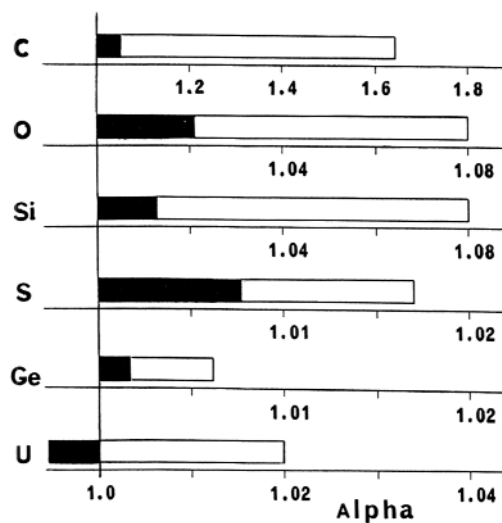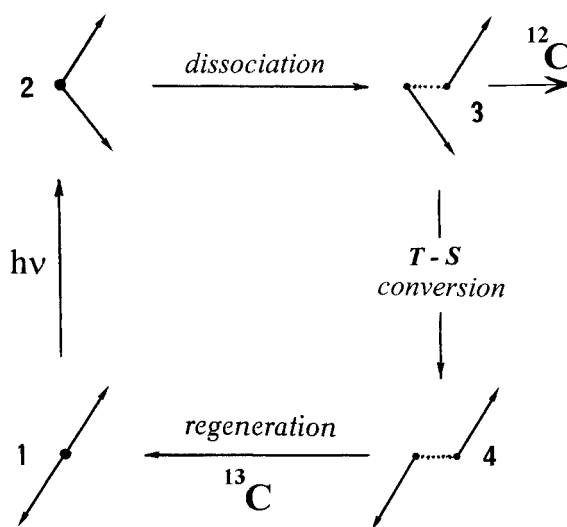
Fig. 9 Scheme of the MIE-induced uranium isotope fractionation.

Fig. 10 One-step isotope enrichment coefficients α. The white fields indicate the range of α values produced by MIE; black fields characterize CIE-induced isotope separation.

Fig. 11 Four-step spin-selective cascade of the photoinduced dissociation–regeneration process.

The most powerful way to increase the recombination probability and, therefore, the cascade parameters, is to localize a reaction in microreactor of confined geometry, such as micelles, zeolite cavities, etc. Cascade theory discloses clearly factors stimulating nuclear spin selectivity and controlling magnetic isotope fractionation. It determines also a hierarchy of the stimulating factors [10]. Priority belongs to the size of the microreactor, which allows it to regulate the molecular dynamics of radical pair and to accommodate it to spin dynamics. According to cascade strategy, microreactors can be considered delicately controlled, nuclear spin-selective devices.

The other powerful strategy to enhance MIE and isotope selection is microwave-induced magnetic isotope effect (MIMIE). The idea of MIMIE was formulated in 1981 and embodied experimentally in 1991 [11,12].

MIMIE is based on the frequency-tuned microwave irradiation, which allows to manipulate with electron spins and to selectively produce triplet–singlet conversion of radical pairs with magnetic and nonmagnetic nuclei. Figure 13 illustrates both of these situations.

Microwave pumping of magnetic pairs stimulates their recombination and significantly increases one-step enrichment coefficient (curve 1). The pumping of nonmagnetic pairs stimulates their recombination and results in decreasing α only at low amplitudes. At high amplitudes ($H_1 \geq 2G$) microwave pumping stimulates coherent precession of both electron spins in radical pair, so that it locks spin dephasing and spin conversion of the pair. It prevents the recombination of nonmagnetic pairs and strongly increases α (curve 2).

Cascade isotope selection

Kinetics   *Statistics*

$$\alpha = \frac{1-P}{1-P*}$$ $$P^n = 1-F$$
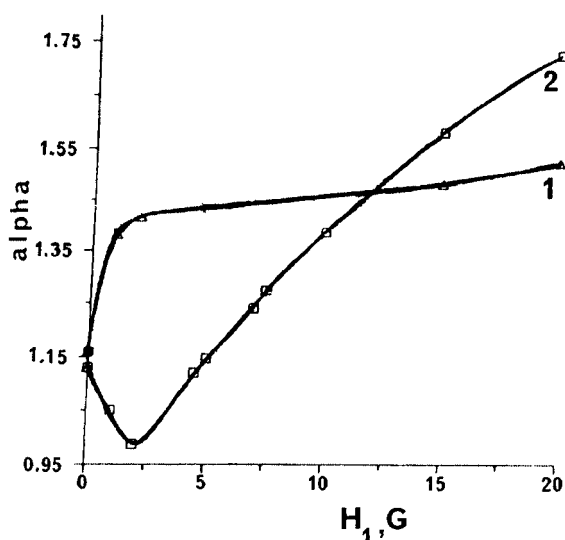
$$\alpha = \frac{ln(1-F)}{ln(1-F*)}$$ $$(P*)^{n*} = 1-F*$$

$$S = \frac{1-F*}{1-F}$$ $$S = (P*)^{n*}/P^n$$

$$\alpha = \frac{n \, ln P}{n* \, ln P*}$$ $$\frac{n*}{n} = \left(\frac{ln P}{1-P}\right) / \left(\frac{ln P*}{1-P*}\right)$$

Fig. 12 The summary of equations characterizing isotope fractionation in partly reversible reactions. The equations are derived from kinetic scheme and cascade statistics respectively.


Fig. 13 Calculated one-step enrichment coefficients α for ^{13}C as a function of microwave field H_1 with pumping of magnetic (1) and nonmagnetic (2) radical pairs of phenacyl and benzyl radicals.

The most efficient regime is expected to be simultaneous microwave pumping of both magnetic and nonmagnetic pairs in order to stimulation the recombination of the former and to suppress that of the latter. Such a cooperation may result in unlimited isotope fractionation.

Experimentally, only the first regime has been tested; microwave pumping of magnetic pairs in the photolysis of dibenzyl ketone enhances isotope effect (Fig. 14). This is the first manifestation of MIMIE in chemistry.

SPIN CATALYSIS

Spin catalysis manifests itself in spin triads. The remarkable and chemically important feature of this new magnetic phenomenon is that the spin conversion of the radical pair (or a pair of any other spin carriers) is induced by nonmagnetic, pairwise exchange interaction between each of the partners of the pair and the third spin carrier. The latter acts as a spin catalyzer, which stimulates spin conversion of the pair. This is a unique, purely physical, catalysis of chemical reactions.
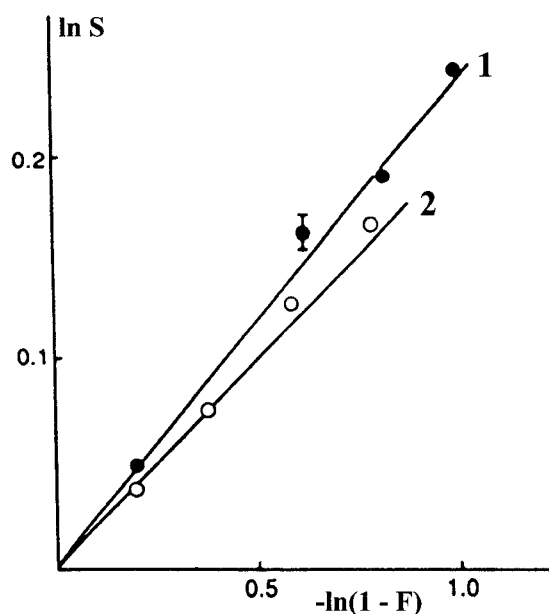
Fig. 14 ^{13}C isotope enrichment as a function of chemical conversion in the photolysis of dibenzylketone with (1) and without (2) microvave pumping.
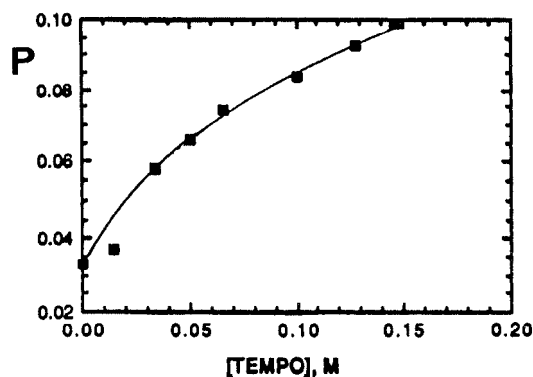
Fig. 15 Recombination probability of the triplet radical pair as a function of TEMPO radical concentration. TEMPO is 2,2,6,6-tetramethylpiperidyl-1-oxyl.

Spin catalysis in spin triads has been detected in many reactions. The recombination of triplet radical pair [PhCH(CH₃)CO   CH(CH₃)Ph] generated by photolysis of d,1-2, 4-diphenyl-3-one was shown to increase three times in the presence of stable nitroxyl TEMPO, when the concentration of TEMPO, which is known to be the powerful radical scavenger, increases from 0 to 0.15 M (Fig. 15).

This result is a direct indication of the spin catalytic effect in radical reactions; it also demonstrates the predominance of the catalytic function of nitroxyls over their traditional function to be a radical scavenger [13].

Another kinetic evidence of catalytic effect has been detected in the recombination of alkyl radicals with nitroxyl biradicals.

$$B + \dot{r} \xrightarrow{\;k_1\;} \dot{M}$$

$$\dot{M} + \dot{r} \xrightarrow{\;k_2\;} \text{product}$$
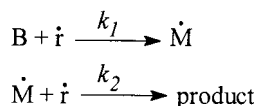
The rate constants of the first recombination of alkyl radical with one of the biradical termini k_1 was shown to exceed those of the second recombination with remaining monoradical terminus k_2 by 10–15%. The effect was attributed to the spin catalysis in the encounter pair of alkyl radical with one of the biradical termini by the second spin-carrying terminus. Taking into account molecular dynamics of the biradical termini (e.g., the dynamics of the reencounters of spins in contact triads) one can estimate the ratio of the rate constants of catalytic and noncatalytic recombination as approximately equals to 10 [14].

The similar spin catalytic effect has been observed in the recombination of triplet radical pair (p-CH₃PhĊH₂   ĊH₂Ph) in micelles in the presence of lanthanide ions as the catalysts. The ratio of the rate constants of catalytic and noncatalytic recombination is a linear function of spin of ions (Fig. 16); this dependence is a direct indication that namely exchange interaction is responsible for the spin catalysis of spin conversion of the pairs under influence of paramagnetic ions. The additional evidence is that there is no dependence of spin catalytic rate constants on the magnetic moment of ions [15].

Cis-trans isomerization of dimethylmaleate into its trans- form, dimethylfumarate, was shown to be strongly accelerated by stable nitroxyl radicals (TEMPO, for instance). Neither decay of nitroxyls nor formation of any byproducts was observed, so this is a case of true paramagnetic catalysis [16]. The rate constants k_0 and k_c of direct and catalytic isomerization are expressed by equations

$$k_0 = 10^5 \exp(-27000/RT), \text{ s}^{-1}$$

$$k_c = 10^{12} \exp(-27000/RT), \text{ s}^{-1}$$

The activation energies of both reactions were shown to be precisely equal, however preexponential factor of catalytic reaction appears to be 7 orders of magnitudes higher than that of direct, non-
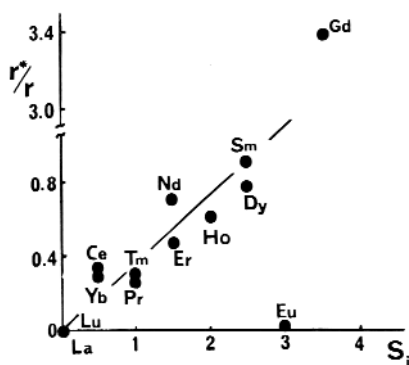
Fig. 16 Ratio of the catalytic/noncatalytic rate constants of the radical pair recombination as a function of spin S_i of lanthanide ions, spin catalyzers.

catalytic reaction. Both these arguments are in favor of "nonmagnetic", purely spin catalysis which is supposed to occur in twisted conformation of the molecule. The pair of π-electrons of double bond in this twisted conformation in cooperation with the third spin of catalyzer may be considered as a spin triad in which spin conversion directs the reaction pathway along the triplet low-lying potential energy surface.

The quantitative hierarchy of spin carriers (radicals, ions, oxygen molecule, etc.) with respect to their spin catalytic efficiency is in excellent agreement with the theory that predicts that the rate of spin conversion in the radical pair has to be proportional to the difference ΔJ of exchange energies between the spin catalyzer and each of the radical pair partners. This statement undoubtedly implies that spin carriers with outer unpaired electrons are much more preferable as spin catalyzer than those with inner unpaired electrons. However, while the former are effective spin catalyzers, they are usually also chemically reactive radical scavengers, whereas the latter, being rather low-efficient spin catalyzers, may be chemically inert. The strategy of spin catalysis is indeed the compromise between these two functions of spin carrier, to be simultaneously spin catalyst and spin scavenger.

The theory of spin catalysis in three-spin system was developed in 1995 [17]. Three spins form 8 spin states; four of them with spin $\frac{3}{4}$ (quartet states) are chemically inert, nonreactive, and do not expose to spin catalysis. Four others with total spin $\frac{1}{2}$ (doublet states) are split into two pairs of states with projections $+\frac{1}{2}$ and $-\frac{1}{2}$ respectively. Spin-catalyzed conversion occurs only in these pairs, with conservation of both total spin and its projection.

Spin-catalyzed conversion can be schematically presented by vector diagram (Fig. 17). Here, R_1 and R_2 denote spins of radical pair partners, R_3 is the third spin of the catalyzer. Exchange interaction of one of the radical partners (say, for instance, R_2) with R_3 results in their precession, which is accompanied by their position exchange. As a result, the pair (R_1, R_2) turns out in singlet state and oscillates between triplet and singlet states. In phase with this oscillation, the third spin of the catalyzer experiences periodically reorientation, so that the total spin and its projection in spin triad remain constant.

Spin oscillations of doublet–doublet, spin-catalyzed conversion obeys equation

$$\rho_s^T(t) = \left(\frac{\Delta J}{2\Omega} \right)^2 Sin^2 \Omega t \tag{4}$$

where ρ_s^T is the probability for the starting triplet pair to appear in singlet state at time t; $\Delta J = J_{13} - J_{23}$, where J_{13} and J_{23} are the pairwise exchange potentials between radical partners (1 and 2) and spin catalyzer 3 respectively;

$$\Omega = \left\{ \frac{1}{2} \left[(J_{12} - J_{13})^2 + (J_{12} - J_{23})^2 + (J_{13} - J_{23})^2 \right] \right\}^{1/2} \tag{5}$$

No oscillations are expected if $J_{12} = J_{23} = J_{13}$; this is a case when spin system is locked.
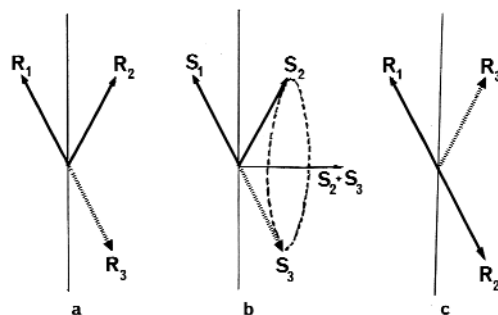
Fig. 17 Vector model demonstrates triplet–singlet conversion of selected radical pair (R_1, R_2), induced by exchange interaction of partners with the third spin of R_3, spin catalyzer.

It is noteworthy that the spin catalysis may also offer an efficient mechanism of nuclear spin selectivity and isotope fractionation [18]. Moreover, in some special circumstances, when the spin triads can be prepared as a spin wavepacket, the quantum beats in chemical transformation of coherent triads may be exhibited [19].

SINGLE-SPIN TUNNELING SPECTROSCOPY

Recent discovery of tunneling electron-vibrational spectroscopy of *single*, *selected molecules* transformed scanning tunneling microscopy (well known as STM), as a topographic method used to monitor atomic and molecular surface relief, into the new powerful technique of chemical physics, which makes feasible to detect *spectroscopy image* of a single molecule, to identify it, and to trace its chemical fate [20].

Physically, the idea of single molecule spectroscopy (SMS) is very simple and beautiful. In autoemissive regime, the tunneling electrons emitted by the tip are locked in the cavity between the tip and the molecule sitting on the surface under the tip. The motion of the electrons in the cavity is restricted by two quantum barriers—on the tip and on the surface molecule (Fig. 18).

In ordinary conditions (tunneling current density $\sim 10^{11}$ electrons/Å^2) the residence time of the electron in cavity is about $10^{-11} - 10^{-12}$ s, so that the cavity functions as a nanoscale resonator, in which standing electron waves are formed; their wavelengths depend on the tip potential. If the wavelength corresponds to that of electron-vibrational level of absorbed molecule then the second, surface quantum barrier becomes transparent and the tunneling electrons penetrate the cavity, so that the tunneling current, which flows between the tip of scanning microscope and the surface on which an adsorbed molecule resides under the tip, has a clear-cut resonance character. The resonance always occurs when the tip potential (and, hence, the energy of tunneling electrons) corresponds to the vibronic level of an adsorbed molecule. Vibrational spectra of single molecules are fingerprints of the molecules under study; more than that, vibrational spectroscopy permits to follow dynamics (residence time) and chemical fate of single molecule. This opens up new prospects for catalysis and surface science.

Single-molecule tunneling spectroscopy provides also new opportunities in detection and monitoring of the single electron spin on the surface (single-spin tunneling spectroscopy, SSTS). The SSTS is based on the physical principles of spin chemistry. In a two-spin system, locked in nanoscale resonator and formed by pair of electrons (one of them is tunneling electron, the second is unpaired electron of the spin carrier under the tip on the surface), there are two spin states—singlet and triplet. This two-spin system is almost identical to radical pair, the partners of which are tunneling (probing) and unpaired (probed) electrons [21].

Energy splitting between these two spin states equals the exchange energy J of electrons in nanoresonator. It means that each of the electron-vibrational levels of the spin carrier under the tip
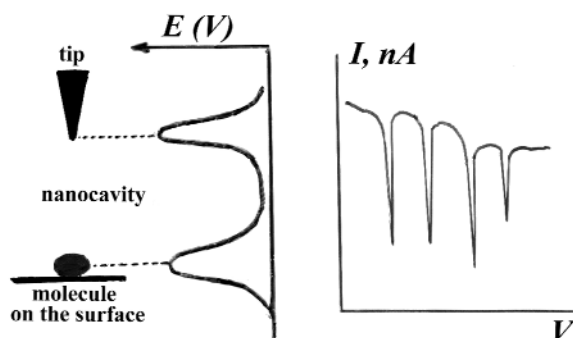

Fig. 18 Schematic presentation of two quantum barriers between the tip and molecule on the surface. The space between barriers is a nanocavity for tunneling electrons.

should be split into the doublets corresponding to singlet and triplet. Nanoresonator is expected to be transparent for the tunneling electrons both in singlet and triplet states, but only at the different energies (different potentials on the tip).

The behavior of the pair of electrons in nanoresonator is identical to that of radical pair. For instance, the recombination reaction

$$\dot{C}H_3 + \dot{O}H \rightarrow CH_3OH$$
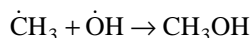
follows along the single channel, while the disproportionation reaction

$$\dot{C}H_3 + \dot{O}H \rightarrow CH_2^T + H_2O$$
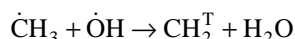
resulting in triplet carbene, occurs in triplet channel. Both reactions are spin allowed because total spin of reagents and products in both reactions is identical, however, their energy cost is different: singlet channel needs no energy, triplet channel meets an energy barrier ~6 kkal/mol. For the pair of electrons in nanoresonator, the energy splitting of triplet and singlet channels equals J.

The first experimental observation of a single spin by STM technique belongs to Dalidchik *et al*. Each line in the vibrational spectrum of O_2^- anion on TiO_2 has been split in doublets (Fig. 19), in perfect agreement with theoretical prediction; the magnitude of the splitting is 0.07 eV [22].

The key parameter measured in this experiment is the exchange energy J of electrons locked in nanocavity. One can be certain that the energy is approximately constant independently of what paramagnetic center sits under the tip; this energy is determined only by the size of nanocavity which, as a rule, only slightly changes in SSTS experiments.

The doublet equidistant line splitting in tunneling spectra is an unambiguous indication of the spin carrier (atom, radical, ion, etc.) under the tip. However, it is impossible to directly identify and discriminate singlet and triplet channels. One can only suppose from general considerations (according to Pauli principle) that the triplet level lies below the singlet one, e.g., the low energy lines of doublets belong to triplet channel, the high energy lines correspond to singlet channel. Further progress in the identification of channels seems to arise from use of ferromagnetic tips.
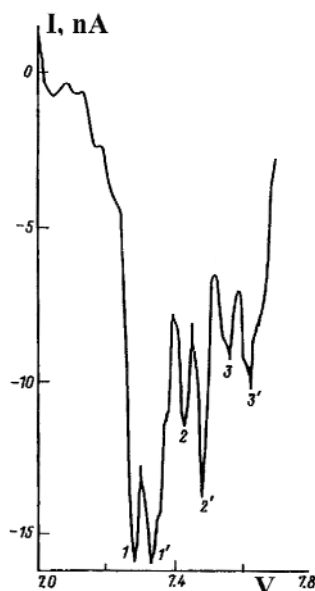
Fig. 19 Tunneling current as a function of tip potential for the single paramagnetic ion O_2^- on the TiO_2 surface. The splitting of vibrational lines (1–1′, 2–2′, 3–3′) is due to exchange interaction in the pair of tunneling and unpaired electrons locked in nanocavity.

As an emitter of spin-polarized electrons, the ferromagnetic tip is expected to provide new opportunities in single-spin tunneling spectroscopy; however, their discussion is beyond the scope of this paper [23].

ACKNOWLEDGMENTS

REFERENCES

1. A. L. Buchachenko, E. M. Galimov, G. A. Nikiforov. *Dokl. Acad. Nauk SSSR* **228**, 379–382 (1976).
2. A. L. Buchachenko. *Chem. Rev.* **95**, 2507–2528 (1995).
3. A. L. Buchachenko. *Progress React. Kinetics* **13**, 163–185 (1984).
4. V. A. Belyakov, E. M.Galimov, A. L. Buchachenko. *Dokl. Acad. Nauk SSSR* **243**, 924–927 (1978).
5. A. L. Buchachenko, L. L.Yasina, V. A. Belyakov. *J. Phys. Chem.* **99**, 4964–4969 (1995).
6. E. N. Step, V. F. Tarasov, A. L. Buchachenko. *Chem. Phys. Lett.* **144**, 523–526 (1988).
7. E. N. Step, V. F. Tarasov, A. L. Buchachenko. *Nature* **345**, 25 (1990).
8. A. L. Buchachenko and I.V. Khudyakov. *Acc. Chem. Res.* **24**, 177–183 (1991).
9. V. Khudyakov and A. L. Buchachenko. *Mendeleev Commun.* **3**, 135–137 (1993).
10. A. L. Buchachenko, V. L. Berdinsky. *J. Phys. Chem.* **A103**, 865–870 (1999).
11. V. F. Tarasov, A. L. Buchachenko, V. I. Maltsev. *Russ. J. Phys. Chem.* **55**, 1921–1926 (1981).
12. V. F. Tarasov, E. G. Bagryanskaya, Y. A. Molin, R. Z. Sagdeev, A. L. Buchachenko. *Mendeleev Comm.* **1**, 85–87 (1991).
13. E. N. Step, A. L. Buchachenko, N. J. Turro. *J. Am. Chem. Soc.* **116**, 5462–5466 (1994).
14. A. L. Buchachenko, E. N. Step, N. J. Turro. *Chem. Phys. Lett.* **233**, 315–320 (1995).
15. A. L. Buchachenko, V. L. Berdinsky, N. J. Turro. *Kinetics and catalysis* (*Russ*), **39**, 325–329 (1998).
16. A. L. Buchachenko and V. L. Berdinsky. *J. Phys. Chem.* **100**, 18292–18299 (1996).
17. A. L. Buchachenko and V. L. Berdinsky. *Chem. Phys. Lett.* **242**, 43–48 (1995).
18. A. L. Buchachenko and V. L. Berdinsky. *Chem. Phys. Lett.* **298**, 279–283 (1998).
19. A. L. Buchachenko and V. L. Berdinsky. *Russ. Chem. Bull.* **9**, 1646–1652 (1995).
20. F. I. Dalidchik, M. V. Grishin, S. A. Kovalevsky, B. R. Shub. *Spectroscopy Lett.* **30**, 1429–1432 (1997).
21. A. L. Buchachenko, M. A. Kozushner, B. R. Shub. *Russ. Chem. Bull.* **47**, 1732–1735 (1998).
22. F. I. Dalidchik and S. A. Kovalevsky. *JETP Lett.* **67**, 965–969 (1998).
23. A. L. Buchachenko, F. I. Dalidchik, B. R. Shub. *Russ. Chem. Rev.*, **71**, 6 (2001).